Thermomechanical analysis of the solidification of fused cast alumina-zirconia-silica refractory blocks

Tiphaine Houdard, Isabelle Cabodi, Pierrick Vespa, Franck Pigeonneau, Charles-André Gandin

Thermomechanical analysis of the solidification of fused cast alumina-zirconia-silica refractory blocks

T Houdard[1,2], I Cabodi[1], P Vespa[1], F Pigeonneau[2] and C-A Gandin[2]

[1] Saint-Gobain, SGR Provence, 84300 Cavaillon, France

[2] Mines Paris, PSL University, CEMEF UMR CNRS 7635, 06904 Sophia Antipolis, France

Abstract. Cooling history of fused cast Alumina-Zirconia-Silica (AZS) refractory blocks is recorded with thermocouples. Postmortem investigations are performed including hot tears. Discussion about solidification path is done with the purpose to better understand phenomena occurring during casting. Heat transfer simulations are compared with recorded temperature histories. Mechanical outputs from THERCAST® are analyzed, revealing the possibility to calibrate the risk of hot tears formation by considering a cumulated strain based criterion.

1. Introduction

Industrial oxide glasses are melted in large tanks at around 1 500 °C. The tank must be durable for up to twenty years. For this reason, alumina-zirconia-silica refractory is commonly used as soldier blocks in the infrastructure of glass furnaces. The fused cast foundry process is used to produce the soldier blocks. It works at extremely high temperatures, typically 1 850 °C. Usual casting defects can be found inside soldier blocks: hot tears along the block edges, macro-porosity in the riser and macro-segregation (or chemical heterogeneity) within the block. Several modeling approaches have been published in the literature to predict hot tear susceptibility in metallic alloys [1, 2]. Despite contributions that focused on thermal stress analyses [3], numerical predictions of hot tears and other defects applied to the fused cast products are still scare.

In the following, the fused cast process is presented in § 2 along with observations. Thenumerical model is briefly presented in § 3. Experimental and numerical predictions are compared in § 4, followed by a discussion in § 5.

2. Fused cast process

Fused-cast ceramic refractory blocks are composed of Alumina (Al_2O_3), Zirconia (ZrO_2), Silica (SiO_2) and Sodium oxide (Na_2O), hereafter referred to as AZS. The material is first melted in an electric-arc furnace before pouring into the sand mold. Block dimensions depend on customer's requirements. A typical block section will be around 0.4×0.25 m^2.

Standard height is around 1.6 m. A block is composed of a rectangular cuboid and a riser above. The block mass is several hundreds of kilograms. Table 1 provides the composition of the AZS refractory material investigated in the current work.

Table 1: Composition of the AZS block.

wt%	Al_2O_3	ZrO_2	SiO_2	Na_2O
AZS41	45	42	12	1

The casting configuration is shown in Figure 1, limited to a quarter of the geometry. In addition to the AZS block (transparent), the casting is composed by the mold (blue) made of sand agglomerated with a resin, an insulating media (orange) controlling the cooling with the environment, a concrete base (brown) holding the mold and the media and a steel bin (red) that contains the entire system.

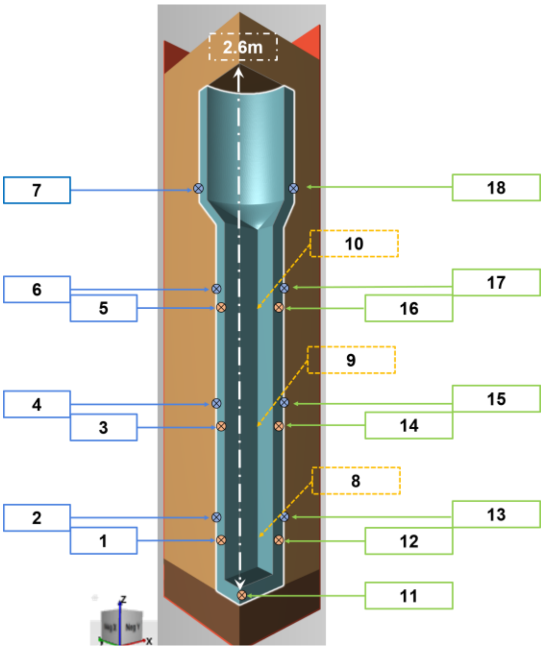

Figure 1: Casting configuration of AZS block (transparent) surrounded by a mold (blue), an insulating media (orange) and a concrete base (brown) contained in a steel bin (red). The 18 thermocouples, installed around the AZS block during an industrial casting, are displayed depending on their position: (orange circle with cross) inside the mold at mid-thickness and (blue circle with cross) outside of the mold. Locations of the thermocouples close to the edge of the block are shown by dashed arrows.

During the cooling period that lasts several days after casting, it is impossible to record temperature inside the AZS itself as liquid temperature is too high for available sensors. Nevertheless, to learn more about the cooling process, temperature inside the mold has been recorded using 18 thermocouples with locations reported in Figure 1. Thermocouples localized inside the mold at mid-thickness are shown with crossed orange symbols while those outside the mold are in crossed blue disks. Position of the thermocouples close to the edge of the block are shown by dashed arrows. The temperature recording is operated every minute and is used to assess the temperature history predicted by numerical simulations.

As already emphasized by Cockcroft *et al* [3], hot tears appear sometimes on the AZS blocks. Such defects are found at the edges of the block. They can extend over few centimeters within the block. An excessively long hot tear can lead to rejection of the block by glass manufacturers. SEM observation of a sample showing an inter-granular crack is presented in Figure 2, with an opening width reaching several hundreds of micrometers.

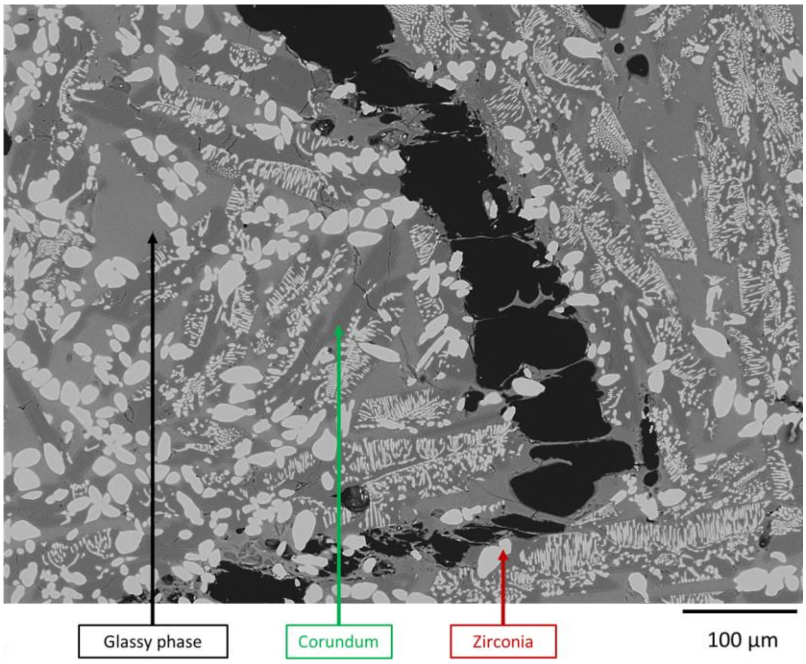

Figure 2: SEM observation of a hot tear showing the presence of glassy strings and the distribution of phases within the various microstructures.

Magnification in Figure 2 reveals the presence of glass filaments inside tears, confirmingthe opening of the crack while liquid phase was still present. No crystal is observed inside theglass filaments. This implies that those cracks occur when the solidification of zirconia andcorundum was over. Micro-probe measurements were achieved all along a hot tear. The glasscomposition was revealed to be similar to the glassy phase composition away from the crack. In complement to this SEM observation, the solidification path is investigated using the Thermo-Calc® software [4] with the TCOX10 database [5]. Roughly, the solidification path inthose conditions is relevant with the SEM observations depicted in Figure 2. Nevertheless, the mullite phase is not observed inside the block while it is expected thermodynamically as thelast phase solidifying from the liquid. Despite the slow cooling process, the casting is too fast to reach thermodynamic equilibrium and the solidification of mullite. The thermodynamic solidification path can therefore be described as follows:

- solidification of 18 wt.% of zirconia from 1 895 °C to 1 759 °C in a tetragonal crystal structure with a dendritic microstructure;
- solidification of additional 29 wt.% zirconia plus 37 wt.% corundum from 1 759 °C to 1 011 °C by forming a two-phase eutectic made of the same tetragonal phase as before plus corundum;
- a martensitic reaction at 1 011 °C, transforming the tetragonal crystal structure into a monoclinic one;
- a glassy phase remains at low temperature, predicted as remaining 16 wt.% “liquid phase”.

3. Thermomechanical simulation

Numerical simulations of the controlled cooling step have been performed with the THERCAST® software [6]. Based on the finite-element method, thermomechanical computation is done by considering the AZS block as a visco-plastic material above a critical temperature, Tc, and as an elasto-visco-plastic material below Tc. The critical temperature controlling the transition between the two behaviors is taken equal to 1 650 °C. Both thermal and mechanical fields are solved with temperature, velocity and pressure as primitive variables [7]. The thermal field is also determined outside the block but those other parts are assumed totally rigid. Properties of the fused-cast ceramic refractory material have been collected through literature [3, 8]. The thermodynamic properties of AZS (density, heat capacity and solidification path) are tabulated with temperature thanks to the TCOX10 thermodynamic database [5]. To agree with observations pointed out in the previous section, tabulations are done by rejecting the mullite phase.

4. Results

4.1. Temperature history

Numerical simulations are computed up to 28 h. Figure 3 displays the temperature as a function of time for the thermocouples #12 and #18 (Figure 1). After pouring, the temperature in the mold reaches its highest values in few hours. Temperature inside the mold is still around 500 °C after 1 day emphasizing that cooling is very slow. At most locations, numerical simulation results, red lines in Figure 3, are in good agreement with experimental data. Nevertheless, important differences between numerical and experimental results are observed in the riser for thermocouple #18 as will be discussed later.

(a) (b)

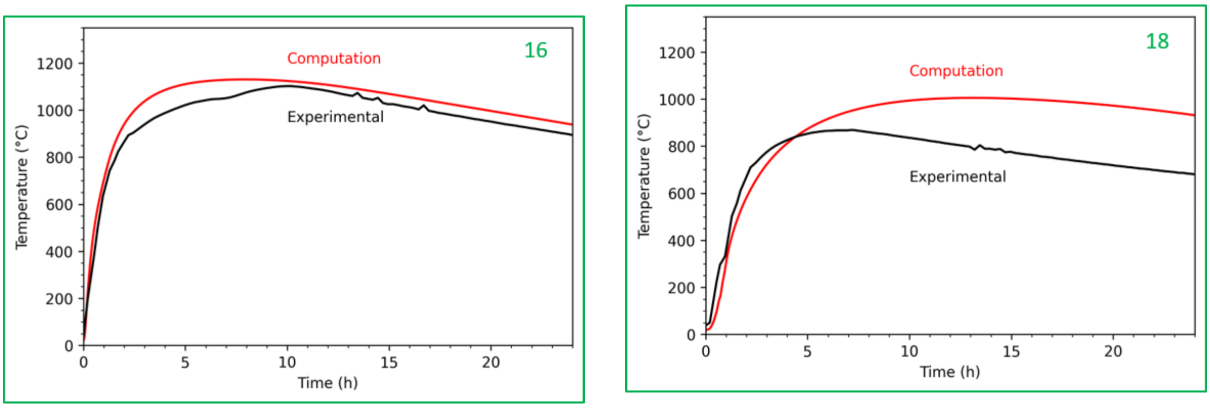

Figure 3: Temperature history as a function of t time for two positions labelled in Figure 1, (a) #16 top of the block, (b) #18 riser. Experimental results (black) are compared to numerical results (red).

4.2. Modeling of hot tear susceptibility

Strain and stress distributions have been modeled in fused cast Alumina refractories [9] and AZS refractories [10]. It is then possible to switch from a strain distribution to a criterion about hot tear susceptibility. For metal alloys, several criteria have been defined to quantify hot tear susceptibility [1, 11]. A hot tear criterion takes into consideration accumulated strain during an interval of temperature that is called Brittle Temperature Range (BTR) $\int_{BTR} \dot{\varepsilon}\ dt$. The BTR is bordered with the zero-strength temperature (ZST) when the remaining liquid is trapped and the zero-ductility temperature (ZDT). The corresponding values hereafter chosen for the BTR are 1 650 °C and 1 300 °C as will be later discussed. Figure 4 shows the distribution of the accumulated strain in a horizontal cross section at height 0.8 m. Such deformation of the block, modeled in THERCAST®, generates strain at the middle of the faces, as shown in Figure 5, where the air layer between the block and the mold is wide. This contraction is anticipated industrially by casting the block with dimensions slightly over the expected standards. Mold combustion is not modeled here and an air gap is created between the mold and the block, that will impact heat exchanges. For the test with Consistency #1, the cumulated strain is maximal along the edge. Numerical sensors are set every 5cm along the edge of the block. Accumulated strain for each sensor is presented in Figure 4b. The distribution is quite similar all along the height of the block, after 24 h, when all sensors have cooled down below 1 300 °C.

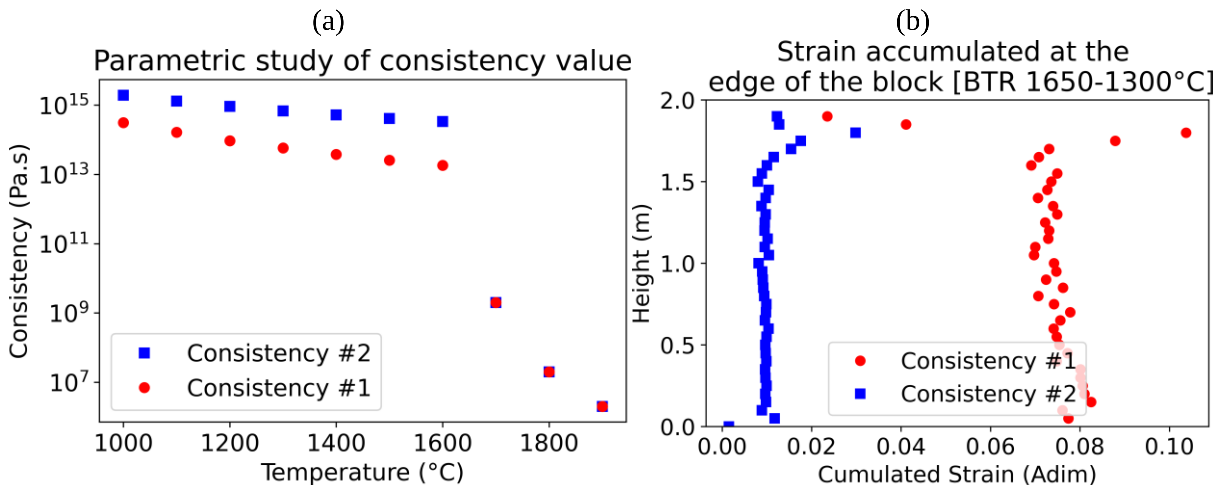

Figure 4: Study of the impact of consistency on sensors along AZS block edge at several heights. (a) tabulations of considered consistencies and (b) Strain cumulated during the range 1 300 °C - 1650 °C at the edge of the block for both consistencies' tabulations

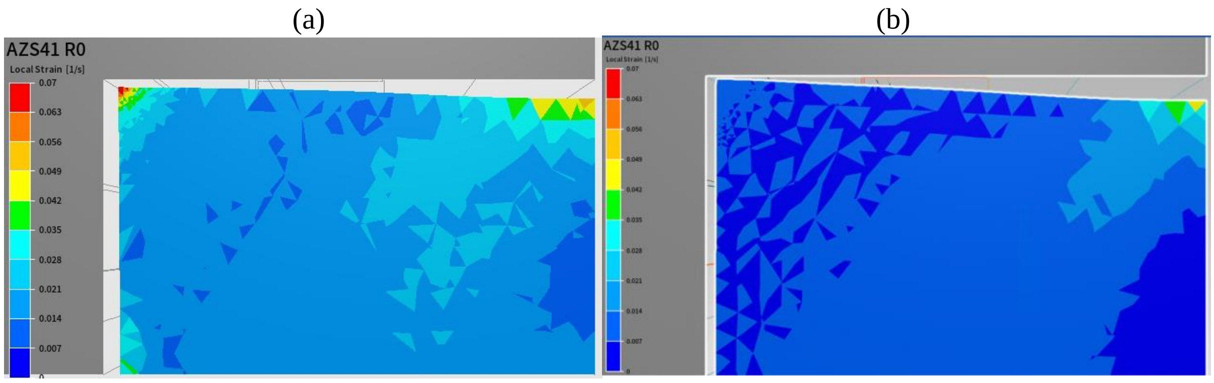

Figure 5: Prediction of Hot Tears Susceptibility inside an AZS block in BTR 1 650 °C to 1300 °C for a block cross section at 0.8 m height that shows also (white) the air gap layer created between the mold (grey) and the accumulated local strain in AZS block (color scale from 0 to 7%) depending on considered consistency: (a) Consistency 1 and (b) Consistency 2.

5. Discussion

5.1. Hot Tears Susceptibility predictions

The BTR is defined for metal alloys between the Zero Strength Temperature (ZST), set as a solid fraction g_s equal to 0.8 [11], and the zero-ductility temperature (ZDT) set at g_s =0.99. For considered refractory ceramics, the solidus is not reached as 15 wt.% of a glassy phase (considered as remaining liquid) is still present at the Glass Transition temperature. An adaptation is therefore required for such cumulated strain criterion. The upper boundary is defined as the temperature when almost all crystals have solidified and remaining liquid composition is very close to the glassy phase composition (i.e. 1 650 °C). The lower boundary is set as 1 300 °C when the liquid viscosity becomes high. The variations of hot tear susceptibility for different industrial cases are retrieved by simulations with this set of parameters.

This criterion is optimized for a given set of parameters. The constitutive equation considered in this article is an additive law considering the effect of strain and strain rate as independent. The considered consistency value is arbitrary lowered at high temperatures when solidification is not over. With such law, the deformation obtained at the edge of the block (in Fig.4b) is quite similar over the height of the block. The top of the block present variations in local accumulated strain that can be related to the time spent in the BTR. Elsewhere, even along the block, the averaged strain is extremely high as the deformation is close to 8 % whereas the critical strain in steel is around 2 % [2]. Validity for such large deformation values is still unclear and the thermo-mechanical properties could justify further investigations.

5.2. Mechanical predictions of shrinkage

After 24h of cooling, the shrinkage due to the solidification is over. Most of the solidificationshrinkage is localized in the riser. Current simulations do not retrieve the temperature history recorded inside the riser (Figure 3b). Also, the riser macro-porosity is predicted much thinnerthan the experimental one. By reducing artificially, the liquid density, solidification shrinkagegets a stronger effect on the riser macro-porosity. If macrosegregation is considered,the liquid inside the riser will be depleted in Zirconia and the density will indeed be lowered.A relevant riser macro-porosity prediction should impact the temperature exchanges with theenvironment.

6. Conclusion

Thermo-mechanical simulations have been run with THERCAST® to determine temperaturehistory and stress/strain distributions during the controlled cooling down stage of an AZS soldier block. Temperature and hot tear susceptibility predictions are in good agreement withmeasurement in the block, except in the riser. Explanations proposed involves the dependenceof thermophysical properties with macrosegregation.

Acknowledgments

This work has been supported by Saint-Gobain Research Provence and the French National Association Research Technology under ANRT CIFRE individual convention of education through research.

References

[1] Bellet M, Cerri O, Bobadilla M, and Chastel Y. 2009. *Metall. Mater. Trans. A*, **40**: pp2705–17.
[2] Won Y M, Yeo T J, Oh K H, and Seol D J. 2000. *Metall Mater Trans B*, **31**: pp779–94
[3] Cockcroft S L, Brimacombe J K, Walrod D G, and Myles T A. 1994. *J. Am. Ceram. Soc.*, **77**(6): pp1505–11.
[4] Andersson J. O., Helander T, Höglund L, Shi P and Sundman B. 2002. *Calphad*, **26**: pp273–312.
[5] Thermo-Calc Software. 2021a. Technical report: TCOX10. Metal Oxide Solutions Database.
[6] Transvalor. Thercast website. https://www.transvalor.com/en/thercast, 2022.
[7] Bellet M, Jaouen O, and Poitrault I. 2005. *Int. J. Numer. Methods Heat Fluid Flow*, **15**(2): pp120 42.
[8] Zhang Y, 2017, PhD thesis. Materials Sciences. PSL Research University.
[9] Au D, Cockcroft S L, and Maijer D. 2002. *Metall. Mater. Trans. A*, **33**: pp2053–65.
[10] Cockcroft S L, Brimacombe J K, Walrod D G, and Myles T A. 1994. *J. Am. Ceram. Soc.*, **77**(6): pp 1512–1521
[11] Yamanaka A, Nakajima K, and Okamura K. 1995. *Ironmaking Steelmaking* **22**(6): pp508–512